The paper was published in the proceedings of the 9th Australia New Zealand Conference on Geomechanics and was edited by Geoffrey Farquhar, Philip Kelsey, John Marsh and Debbie Fellows. The conference was held in Auckland, New Zealand, 8 – 11 February 2004.

Wave-Induced Liquefaction Around A Buried Pipeline

L. Cheng
Department of Civil and Resource Engineering, The University of Western Australia
B.M. Sumer and J. Fredsoe
Coastal and River Engineering Section, Technical University of Denmark
Y. Hu
Department of Civil Engineering, Curtin University of Technology, Western Australia

Summary: A two-dimensional modified Biot consolidation equation with a source term is solved for residual pore pressure around a buried pipe. The source term representing the rate of pore pressure accumulation is empirically established based on the ratio of initial shear stress to initial normal stress. The initial shear stress is calculated by solving the governing equations of flow of a compressible pore fluid in a compressible porous medium, in the presence of the pipe. The surface of the pipe is assumed to be either completely smooth or completely rough. It is found that the pore pressure accumulation around the pipeline is affected by the initial shear stress distributions. The numerical results are compared with wave tank test results. It is found that the numerical model predicts the pore pressure accumulation in a uniform layer of soil well but is not very successful with the pore pressure accumulation around the pipe.

INTRODUCTION

Research efforts have been devoted to the study of the stability of a buried pipeline. Early research on the stability of a buried pipeline can be dated back to the pipe floatation investigation carried out by the ASCE Pipeline Floatation Research Council (1966). It was observed that the pipeline either floated or sank if the soil was liquefied, depending on the specific gravity of the soil and the pipe. Silvis (1990) reported a study where liquefaction potential has been assessed for an 810 km long and 1.25 m diameter gas line laid from Sleipner in the North Sea to Zeebrugge on the Belgian coast. de Groot and Meijers (1992) presented an investigation on the risk of the floatation of the pipeline laid in a trench that was back-filled with local sand. Siddharten and Norris (1993) conducted a numerical analysis of pipeline floatation under North Sea wave and soil conditions.

More recently Sumer et al. (1999) reported an experimental study on the sinking and floatation of pipelines in liquefied soils under waves. In that study, experiments were carried out to investigate the sinking and floatation of pipelines and other objects in a silt bed. It was found that the pore water pressure in the silt bed built up progressively under a progressive wave. The soil was liquefied for wave heights larger than a critical value. It was also found that the pipe with a relatively small specific gravity floated to the surface of the soil due to wave-induced liquefaction.

Numerical study on pore pressure accumulation around a buried pipe is rare. There are however some studies investigating the harmonic wave-induced pore pressure around a buried pipe. Cheng and Liu (1986) investigated the pore pressure and uplift forces on a pipe buried in a region that was surrounded by two impermeable walls. Magda (1997) examined a similar case but with a wider range of degrees of saturation. Jeng and Cheng (2000) investigated the wave-induced instability of a buried pipe in a soil obeying the Mohr-Coulomb failure criterion. More recently Sumer and Cheng (1999) examined the potential of liquefaction around a buried pipe using a random walk method. Cheng et al. (2001) investigated the pore pressure accumulation in the seabed due to progressive waves.

The purpose of the present study is to develop a numerical model of wave-induced pore pressure accumulation around pipelines buried in the seabed. The numerical model solves the two-dimensional modified Biot consolidation equation (with a source term) for the pore pressure accumulation, following a similar approach reported by Rahman et al. (1977). The initial shear stress is calculated by solving the governing equations of flow of a compressible pore fluid in a compressible porous medium (Jeng and Cheng 1999), with the presence of the pipe.

BASIC EQUATIONS

The two-dimensional governing equation of the period-averaged excess pore pressure in a homogeneous, isotropic soil can be derived from the two-dimensional Biot consolidation equation as (Rahman et al., 1977):

$$\frac{\partial p(x,z,t)}{\partial t} = c_v \nabla^2 p(x,z,t) + f(x,z,t) \qquad (1)$$

where $p(x,z,t)$ represents the period averaged pore pressure, t is time, x and z are the horizontal and vertical coordinates as shown in Fig.1, ∇^2 is the Laplace operator, $f(x,z,t)$ is a source term representing the rate of pore pressure build up, and c_v is the consolidation coefficient given as

$$c_v = \frac{Gk}{\gamma_w}\frac{2-2\nu}{(1-2\nu)+(2-2\nu)\beta n' G} \tag{2}$$

Here ν is the Poisson's ratio, G is the soil shear modulus, k is the permeability of the soil, γ_w is the unit weight of the pore fluid, n' is soil porosity, and β' is the effective compressibility of the pore fluid and is defined as

$$\beta' = \frac{1}{K_w} - \frac{1-S_r}{P_{w0}} \tag{3}$$

In eq. (3), K_w is the true bulk modulus of elasticity of water (taken as 2×10^9 N/m^2). P_{w0} is the absolute pore water pressure (it can be taken as the initial value of pore water pressure), and S_r is the degree of saturation.

Eq. (1) is solved in a domain as shown in Fig. 1, together with the following initial and boundary conditions:

$$p(x,z,0) = 0 \tag{4}$$

$$p(x,0,t) = 0 \tag{5}$$

$$\frac{\partial p(x,d,t)}{\partial z} = 0 \tag{6}$$

$$\frac{\partial p(x,z,t)}{\partial n}\bigg|_{pipe} = 0 \tag{7}$$

$$p(x,z,t) = p(x+L,z,t) \tag{8}$$

where n is the normal direction to the pipe surface and L is the wave length. Here, Eq.(4) states that the calculation starts with a zero average pore pressure everywhere, Eq. (5) implies a zero period-averaged pressure at the mudline, Eq.(6) means an impermeable bed at soil depth d, and Eq.(7) represents the no-flow in or out of the pipe. Eq. (8) is the periodic boundary condition at the lateral boundaries. Eq. (8) also implies that the length of the calculation domain is always taken as one wavelength.

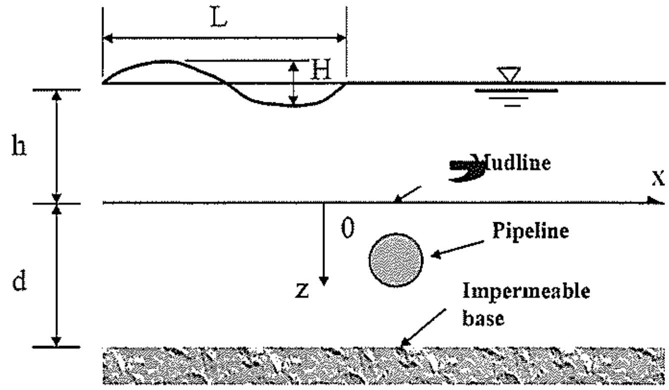

Fig. 1 Definition sketch

The source term in Eq. (1) represents the pore pressure generation rate. It normally depends on the relative density of soil, initial and cyclic shear stress ratios, and the existing pore pressure already built up by previous cycle (Rahman, et al., 1977). The derivation of this term can be found in many places (e.g. Seed and Rahman, 1978; McDougal et al., 1989) and will not be repeated here. For a linear relationship between the pore pressure ratio and the cyclic ratio, this term can be expressed as

$$f = \sigma_0'\left(\frac{1}{\alpha}\frac{\tau_{xz}}{\sigma_0'}\right)^{-1/\beta}\frac{1}{T_w} \tag{9}$$

Here T_w is the wave period, σ_0' is the initial effective normal stress, τ_{xz} is the amplitude of cyclic shear stress in the soil, and α and β are the curve-fitting coefficients (depending on N_l, the number of cycles leading to liquefaction). The initial effective normal stress can be taken as (McDougal et al., 1989)

$$\sigma_0' = \gamma' z\frac{1+2k_0}{3} \tag{10}$$

where γ' is the submerged specific weight of soil and k_0 is the coefficient of the lateral earth pressure.

NUMERICAL SOLUTION

The governing equation, Eq. (1), for pore pressure accumulation, together with the initial and boundary conditions, Eqs (4) – (8), is solved numerically by using the finite difference method in a curvilinear coordinate system. The use of Crank-Nicolson's scheme and a central-difference for all other derivatives guarantees that the solution is of second-order accuracy both in time and space.

It can be seen from equation (1) and (12) that the pore pressure accumulation in the soil depends on the initial shear stress ratio in the soil. For the two-dimensional case considered here, the initial shear stress is calculated by solving the Biot consolidation equations with the presence of the pipe. The details of such a solution can be found in Jeng and Cheng (2000).

RESULTS AND DISCUSSIONS

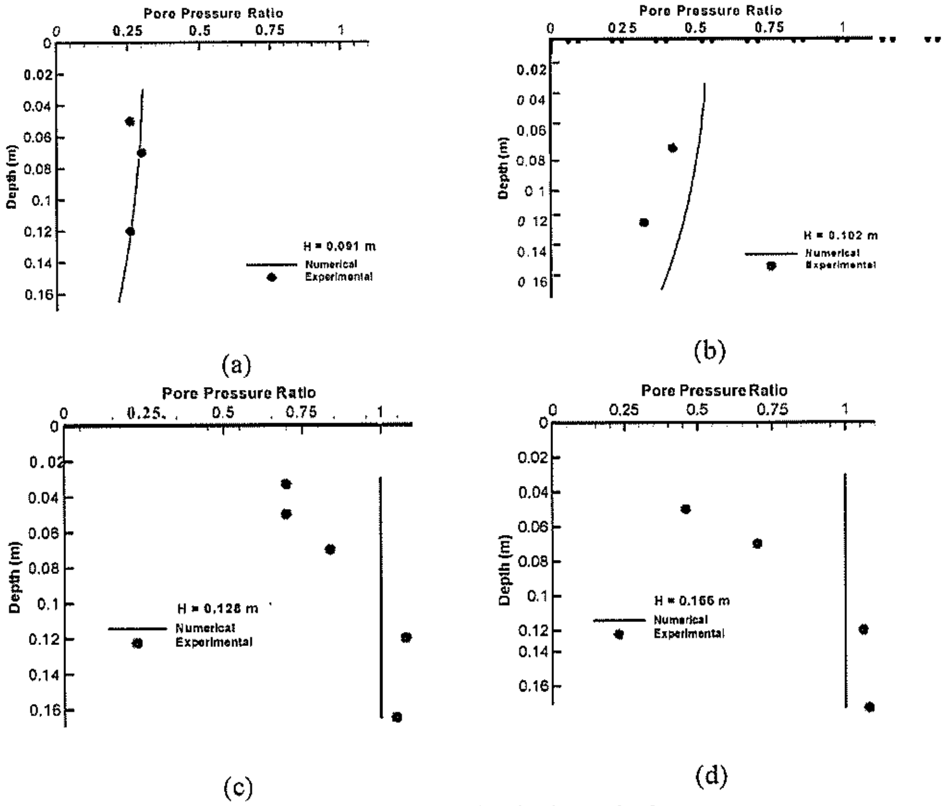

Fig. 2 Equilibrium pore pressure accumulation in the seabed

Pore pressure accumulation in a uniform layer of soil

To validate the numerical method used in this study, the numerical model is applied to calculate pore pressure accumulation in a uniform layer of soil of 0.17m, subject to progressive waves. For the purpose of comparison, the soil and wave conditions employed in the calculation are the same as those measured in the tests (Sumer et al., 1999) and are given in Table 1 and Table 2, respectively.

The calculations are carried out in a rectangular domain of 2.894×0.17 m with the absence of the pipe. The domain is discretized using a 79x69 mesh after a careful grid dependence study. The calculations are marched in time till the steady solution has been reached for the soil and wave conditions outlined in Table 1 and Table 2. The time-step used is 1.6 seconds.

The numerical results of the steady pore pressure ratio ($p(z)/\sigma_0'$) in the soil layer are given in Fig. 2, together

Table 1 Approximate Soil Conditions

Poisson's ratio	0.35
Shear modulus (kN/m^2)	540
Submerged weight (kN/m^3)	10.73
Permeability (m/s)	5.37×10^{-8}

Table 2 Wave Conditions (after Sumer et al., 1999)

Test case	1
Wave period (s)	1.6
Wave height (m)	0.091
Water depth (m)	0.42
Soil depth (m)	

with the experimental results of Sumer et al. (1999). The wave heights investigated are 0.091m, 0.102m, 0.128 m and 0.166 m. Pore pressure ratio of 1.0 in the figure corresponds to soil liquefaction. It can be seen from Fig. 2(a) and Fig. 2(b) that the numerical result agrees well with the experimental measurement for smaller wave heights where the soil is not liquefied. For the higher wave heights (Fig. 2(c) and Fig. 2(d)), although the measured pore pressure was slightly less than the overburden pressure, the soil liquefaction across the entire layer of soil was observed in the experiments (Sumer et al. 1999). This agrees with the present numerical results.

Fig. 3 shows the pore pressure accumulation with time at three different depths inside the soil at different wave heights. The following two aspects are obvious from the figure. First of all, the numerical model generally predicts the steady accumulated pressure well as demonstrated in Fig.2. Secondly, the predicted time required to liquefaction is significantly larger than those observed in experiments for the cases where the soil is actually liquefied (please refer Sumer et al. 1999). It is found in the calculations that the time required to liquefaction is sensitive to the values of a and β used in Eq. (9). The values of a and β used in the calculation are determined by curve-fitting the curves of Alba et al. (1976) for the relative density *Dr* reported by Sumer et al. (1999). The applicability of the curves by Alba et al. (1976) to the present soil conditions is not very clear and needs to be further investigated.

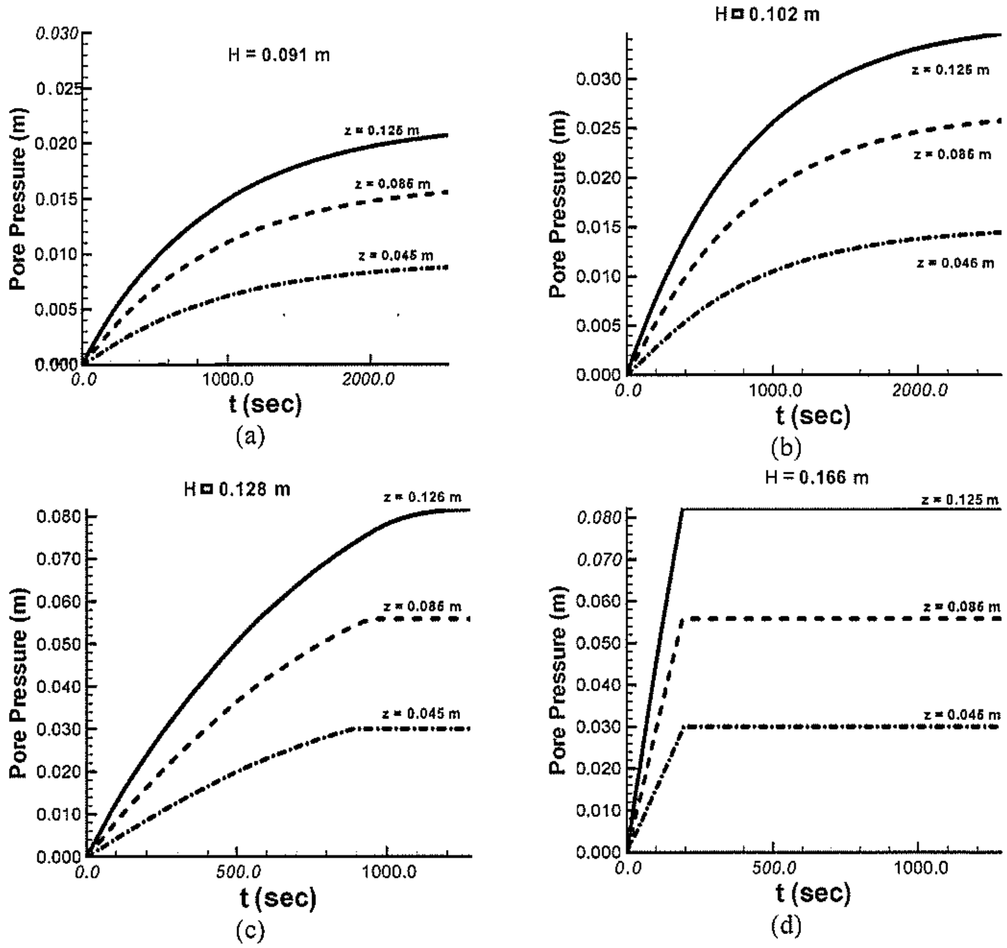

Fig. 3 Transient pore pressure accumulation in the seabed

Pore pressure accumulation around a buried pipe

To validate the numerical models, the test cases in an experimental study of pore pressure accumulation around a buried pipe (Sumer et al. 2003) are calculated using the present numerical models. In the tests of Sumer et al. (2003), an 8 cm pipe is buried in a uniform layer of soil of 17 cm. The center of the pipe is located at middle of the soil layer. The same soil and wave conditions as those given in Table 1 and Table 2 are also used in the tests as well as in the calculations. The numerical results of a smooth pipe and a rough pipe are compared with the experimental results.

Smooth pipe

For the smooth pipe case, the initial shear stress will be calculated by solving Eqs. (13), (20) and (21), together with the corresponding boundary conditions. The resolved shear stress field will be used in Eq. (12) to calculate the source term *f* for pore pressure accumulation in the soil.

Fig. 4 shows the local shear stress distribution around a smooth pipe. The solid lines are the initial shear stress contours with the presence of the pipe and the dashed lines are the undisturbed shear stress contour lines. It can

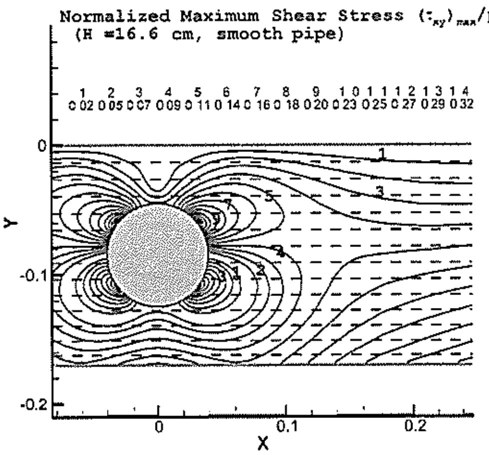

Fig. 4 The maximum shear stress ratio for a smooth pipe with H = 16.6 cm

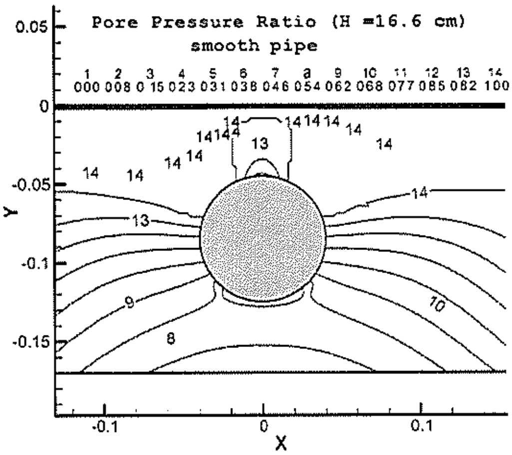

Fig. 5 The equilibrium pore pressure ratio for a smooth pipe with H = 16.6 cm

be seen clearly that there are two zones of shear stress concentration and amplification on the top shoulders of the pipe. The maximum shear stress amplification is about a factor of 3 and takes place near the pipe surface. In the two zones at the lower shoulders of the pipe, the shear stress is lower than the undisturbed counterpart. This is likely due to the sheltering effect of the pipe. The shear stress values directly at the top and bottom of the pipe are smaller than the undisturbed shear at the same locations. Fig. 5 shows the corresponding ratio of pore pressure to overburden pressure (referred to as pore pressure ratio) around the pipe when the steady state solution is reached. It can be seen that the soil near the two top shoulders of the pipe liquefied as the result of the higher shear stress ratio in these zones. The soil in the other near pipe regions is not liquefied as the result of the smaller shear stress ratio, in contrast to the liquefied soil in the zones far away from the pipe. It can be seen that the predicted distribution of the pore pressure ratio agrees with the normalized shear stress ratio given in Fig. 4.

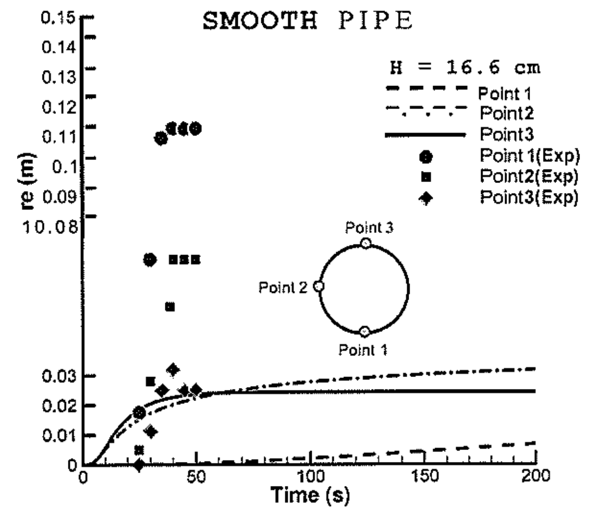

Fig. 6 The pore pressure accumulation for a smooth pipe subject to waves of H = 16.6 cm

Fig. 6 shows the predicted time history of pore pressure accumulation at three points on the pipe, together with the experimental results of Sumer et al. (2003). It should be noted that the experimental results given in Fig. 6 are the period averaged pore pressure. It is seen from Fig. 6 that the predicted pressure on the top of the pipe increases rapidly and reaches to a constant value that is slightly lower than the over burden pressure (0.03m). This seems to agree with the experimental result, although the speed of pore pressure accumulation in the tests (Sumer et al. 2003) is higher. The predicted pressure at the bottom of the pipe rises very slowly, in contrast to the rapid increase in the experiments. The predicted pore pressure at the middle point (point 2) accumulates almost as fast as the top point but its equilibrium value is much more smaller than that measured in the tests.

The calculations are also carried out for other wave heights and the results are very similar to those given in Fig.6. The numerical results at point 2 and point 3 do not agree with the experimental results very well. The reason for discrepancy is not very clear. It is speculated that the discrepancy is due to uncertainty with regard to the calculated shear stress ratio in the region below the pipe. The actual over burden pressure below the pipe in the tests may be smaller than that calculated using Eq. (10). It is speculated that a small gap between the pipe and the soil underneath the pipe might exist, given that the pipe was fixed to the flume walls and the soil was quite loss packed initially. However this needs to be further verified.

Rough pipe

Fig. 7 shows the pore pressure ratio around the pipe when the steady state solution is reached. It can be seen that the soil on the top of the pipe is liquefied as the result of high shear stress ratio in this region. The soil in the other near pipe region is not liquefied as the result of the relatively low shear stress ratio. Fig. 8 shows the predicted time history of pore pressure accumulation at three points on the pipe, together with the experimental results of Sumer et al. (2003). It is seen from Fig. 8 that the predicted pressure on the top of the pipe increases

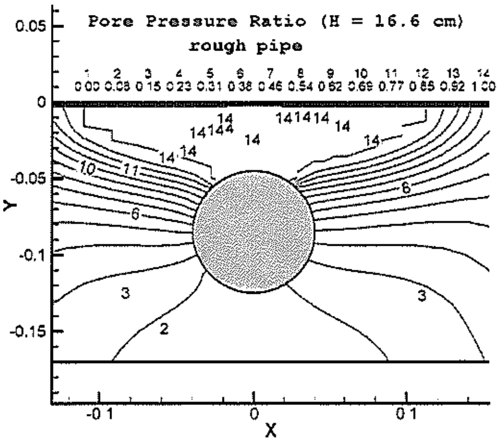

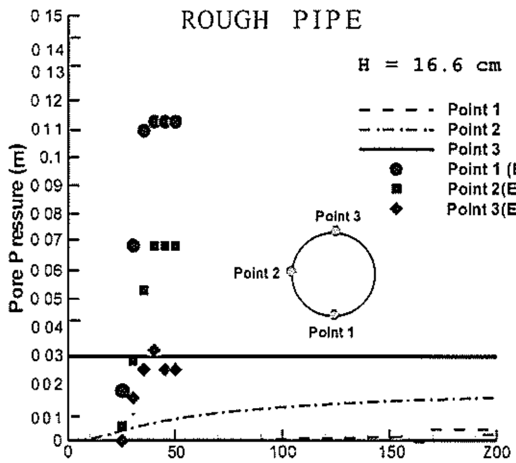

very sharply and then reaches to the over burden pressure (≈ 0.03m). This indicates that soil on top of the pipe liquefied straightaway as the wave propagates over the seabed. The predicted pressure at point 2 and the bottom of the pipe increase slowly and reach to constant values. The comparison of the numerical results with the experimental results for the rough pipe is very similar to the smooth pipe case. The calculations carried out for other wave heights for the smooth pipe indicated the similar trends. It can be seen that the roughness of pipe does not significantly influence the pore pressure accumulation around the pipe.

CONCLUSIONS

A numerical model for pore pressure accumulation around a buried pipe is developed in this paper. The numerical model solves a two-dimensional modified Biot consolidation equation (with a source term) for the pore pressure accumulation. The initial shear stress field that is needed for pore pressure accumulation is calculated by solving the governing equations of a compressible pore fluid flow in a compressible porous medium around a smooth pipe and a rough pipe. The comparison of the numerical results with experimental results allows the following conclusions to be drawn:

1. The present model works well for wave-induced pore pressure accumulation in an uniform layer of soil;
2. The calculation results are sensitive to the α and β coefficients that are used in the source term in the Biot equation. It is suggested the coefficients need to be determined for the local soil conditions;
3. The predicted pore pressure at the top of the pipe agreed well with the experimental results but disagrees at other points. The reason for the discrepancy needs to be discovered.
4. The roughness of the pipe surface does affect the pore pressure accumulation around the pipe but not significantly.

ACKNOWLEDGEMENT

The major part of this work was carried out while the first author was on sabbatical leave at Department of Hydrodynamics and Water Resources (ISVA), Denmark Technical University. The first author is very grateful for the study leave grant from The University of Western Australia and the support from a UWA research grant.

This study is also supported partially by the Commission of the European Communities, Directorate-General XII for Science, Research and Development FP5 Program Contract No. EVK3-CT-2000-00038 Liquefaction Around Marine Structures (LIMAS), and by the five-year (1999-2004) Framework Programme "Computational Hydrodynamics" of the Danish Technical Research Academy, STVF.

REFERENCES

Alba, P. D., Seed, H. B. and Chan, C. K. (1976), "Sand liquefaction in large-scale simple shear tests". J. of the Geotechnical Engineering Division, ASCE, Vol. 102, No. GT9, 909-927.

ASCE Pipeline Floatation Research Council (1966), "ASCE preliminary research on pipeline floatation." ASCE J. Pipeline Division, Vol. 92, No. PL1, pp. 27-71.

Cheng, H.-D. and Liu, P. L.-F. (1986). "Seepage force on a pipeline buried in a poroelastic seabed under wave loading." Applied Ocean Research, Vol. **8**, No. 1, 22-32.

Cheng, L., Sumer, B. M. and Fredsoe. J. (2001). "Solutions of pore pressure accumulation due to progressive waves." Int. J. Numerical And Analytical Methods in Geomechanics, *25*, 885-907.

de Groot, M. B. and Meijers, P. (1992), "Liquefaction of trench fill around a pipeline in the seabed." BOSS 92, Behaviour of Offshore Structures, London, 1333-1344.

Jeng, D.-S. and Cheng, L. (2000), "Wave-induced seabed instability around a buried pipeline in a poro-elastic seabed." Ocean Engineering, Vol. 27, 127-146.

Magda, W. (1997). "Wave-induced uplift force on a submarine pipeline buried in a compressible seabed." Ocean Engineering, Vol. 24, No. 6, 551-576.

McDougal, W. G., Tsai. Y. T., Liu. P. L-F and Clukey, E. C. (1989), "Wave-induced pore water pressure accumulation in marine soils," Trans. ASME, J. Offshore Mechanics and Arctic Engineering, Vol. 111, 1-11.

Rahman, M. S., Seed, H. B. and Booker, J. R. (1977). "Pore pressure development under offshore gravity structures," Journal of the Geotechnical Engineering Division, ASCE, Vol. 103, No. GT 12, 1419- 1437.

Seed, H. B. and Rahman, M. S. (1978), "Wave-induced pore pressure in relation to ocean floor stability of cohesionless soil." Marine Geotechnology, 3, No. *2*, 123-150.

Silvis, F. (1990). "Wave induced liquefaction of seabed below pipeline." The 4th Young Geotechnical Engineers' Conference, Delft, The Netherlands, 18-22 June 1990.

Sumer, B. M. and Cheng, N.-S. (1999), "A random-walk model for pore pressure accumulation in marine soils." The 9th International Offshore and Polar Engineering Conference, ISOPE-99, Brest, France, May 30-June 4, 1999.

Sumer, B. M., Fredsoe, J., Christensen, S and Lind, M. T. (1999). "Sinking/floatation of pipelines and other objects in liquefied soil under waves," Coastal Engineering 38, 58-90.

Sumer, B. M. and Cheng, N. S. (1999), "A random-walk model for pore pressure accumulation in marine soils," The 9th International Offshore and Polar Engineering Conference, ISOPE-99, Brest, France, Vol. 1, 521-528.

Sumer, B.M., Truelsen, C. and Fredsoe, J.: "Liquefaction around pipelines under waves". Paper to be submitted to Coastal Engineering.